

Generalized three body problem and the instability of the core-halo objects in binary systems

Andrzej Odrzywolek*

M. Smoluchowski Institute of Physics, Jagiellonian University, Reymonta 4, 30-059 Krakow, Poland

29 March 2022

ABSTRACT

Goal of the presented research is to construct simplified model of the core-halo structures in binary systems. Examples are provided by Thorne-Zytkov objects, hot Jupiters, protoplanets with large moons, red supergiants in binaries and globular clusters with central black hole. Instability criteria due to resonance between internal and orbital frequencies in such a systems has been derived. To achieve assumed goals, generalized planar circular restricted three body problem is investigated with one of the point masses, M , replaced with spherical body of finite size. Mechanical system under consideration includes two large masses m and M and the test body with small mass μ . Mass μ , initially, is placed in the geometric center of mass M , and shares its orbital motion. Only gravitational interactions are considered, and non-point mass M is assumed to be rigid with rotational degrees of freedom neglected. Equations of motion are presented, and linear instability criteria are derived using quantifier elimination.

Motion of the test mass μ is shown to be unstable due to resonance between orbital and internal frequencies if $\frac{M}{d^3} < \frac{4}{3}\pi\rho < \frac{M+3m(1+\mu/M)^{-1}}{d^3}$, where ρ is the central density of mass M , and d distance between masses m and M (circular orbit diameter). In the framework of model, the central mass μ can be ejected if resonance conditions are met during the evolution of the system. The above result is important for core-collapse supernova theory, with mass μ identified with helium core of the exploding massive star. The instability cause off-center supernova "ignition" relative to the center-of-mass of the hydrogen envelope. The instability is also inevitable during protoplanet growth, with hypothetical ejection of the rocky core from gas giants and formation of the "puffy planets" due to resonance with orbital frequency. Hypothetical central intermediate black holes of the globular clusters are also in unstable position with respect to perturbations caused by the Galaxy. For sake of curiosity I note, that the Earth-Moon, and the Earth-Sun systems are stable in the above sense, with test body μ being the artificial black hole created in the failed high-energy physics experiment.

Key words: Physical data and processes: gravitation, instabilities, chaos — Astrometry and celestial mechanics: celestial mechanics — Planetary systems: planets and satellites: dynamical evolution and stability, formation, planet-star interactions — Stars: binaries: general, supergiants, kinematics and dynamics

1 INTRODUCTION

Traditional classical mechanics approach to astrophysical binaries usually assume that mechanical system can be described in terms of point masses. However, in many important situations, this assumption is broken, e.g., the motion of the spacecraft in the gravitational field of the non-spherical asteroid (Wang and Xu 2013), require more general description (Hur e and Dieckmann 2012). In astrophysics, we frequently have to deal with core-halo objects. These bodies still possess spherical symmetry. Total mass is unevenly divided into nearly point-like central object, and extensive, low-density envelope.

For example, all red-giants are composed of small, high-density helium core, surrounded by a huge low-density envelope (Woosley et al. 2002). Noteworthy, mass of the envelope is usually dominant, and vary by order of magnitude from few solar masses up to $\sim 100 M_{\odot}$. On the contrary, mass of the helium core is roughly 4-5 M_{\odot} for all stars.

Gaseous giant planets ("Jupiters") are composed of the rocky core and extended envelope. Inside icy moons (e.g. Europa, Enceladus) and exoplanets ("blue ocean" super-earths, see Haghighipour 2011) we also find rocky core, this time "floating" in the surrounding liquid ocean (Kuchner 2003; L eger et al. 2004). Therefore, in some situations, aforementioned bodies should be treated as two-component structures.

Globular cluster (GC) with central intermediate-mass black

* E-mail: andrzej.odrzywolek@uj.edu.pl

hole (IMBH, see Umbreit and Rasio 2013; Sun et al. 2013; Feldmeier et al. 2013; Lützgendorf et al. 2013a,b,c,d) is another very important case of the core-halo object. Noteworthy, non-gravitational effects are essentially negligible in GC-IMBH system, providing perfect testbed for presented theory.

There are also more exotic examples. Thorne and Zytlow (1977) object, composed of central neutron star or black hole and normal star provides illustrative case (Vanture et al. 1999; Cannon 1993; Cannon et al. 1992). Yet another example is the non-standard Solar model with black hole inside (Hawking 1971; Clayton et al. 1975). Artificial black hole created on Earth in failed high-energy experiment (Casadio et al. 2010; Bleicher and Nicolini 2010; Gingrich 2010) also would lead to creation of the core-halo system.

The big question is, what if the core-halo system is a part of orbiting gravitationally bound system? For red giants, it would be a binary companion star. For planets: moons, and *vice versa*. For globular clusters, it is the host Galaxy. In all above examples, binary interaction effects are known to be non-negligible, e.g., tidal interactions. In extreme cases, mass transfer or a total disruption of one component is possible. Are there other types of instability, resonant in particular? I try to answer this question in the framework of mechanical model.

Original motivation for creation of presented model is suggestion of Arnett and Meakin (2011), that in core-collapse supernovae iron core might be displaced with respect to geometrical symmetry center of the extended and usually much more massive hydrogen envelope. Arnett and Meakin (2011) proposed hydrodynamical $L=1$ instabilities during Si burning as a main cause of the displacement. Arnett and Meakin (2011) wrote: „*If there were a driving mechanism for core-mantle oscillation, here would be an asymmetry due to the displacement of the core and mantle relative to the center of mass.*” Here I propose another mechanism: gravitational instability in binary core-halo system.

The point mass in the center of an extended object would oscillate, if it was perturbed (displaced) from central position. Is this position stable with respect to perturbations caused by the third body orbiting outside? Naively, one might expect, that it is always possible to tune internal frequency and orbital frequency. However, we are dealing with energy-conserving system. Many years of struggle to answer very similar questions in the classic three body problem (Mardling 2008a) suggest caution, and rigorous mathematical approach.

The article is organized as follows. In Sect. 2 details of the model created to describe core-halo system in binary are presented. Approach based on restricted planar circular three body problem (thereafter RPCTBP) has been presented in Subsect. 2.1, together with linear stability analysis for uniform density ball. Subsection 2.2 contains numerical verification of the results, and behavior in non-linear regime. In Subsect. 2.3 much more general model with non-planar motion and third body of finite mass μ is provided. Potential astrophysical sites of the instability are presented in Section 3: massive pre-supernova stars (Subsect. 3.1), (exo)planets and moons (Subsect. 3.2) and globular clusters with IMBH (Subsect. 3.3). Importance of instability, limitations of mechanical model, chances for observational verification and directions of future research are summarized in concluding Sect. 4.

2 DERIVATION AND NUMERICAL VERIFICATION OF THE INSTABILITY CRITERIA

2.1 Restricted planar circular three body problem approach

To handle dynamics of the core-halo object in binary system, the following model has been created. Mechanical system of interest (cf. Fig. 1) includes two masses m and M orbiting the center of mass on circular orbits. Mass m (first body) is a point mass. Mass M (second body) is extended spherical body with known density $\rho(r)$. The body with mass M is rigid. Rotational degrees of freedom for mass M are not considered, though. Third body is a test body, so its mass is assumed to be negligible (see Subsect. 2.3 for more general model with this assumption relaxed). In this subsection only, in order to simplify formulae, and facilitate derivation of linear instability criteria, I further assume that density $\rho(r)$ inside mass M is constant and equal ρ . Additionally, mass m is assumed to orbit outside radius R of mass M . This allows us to use classic RPCTBP formulae. Distance between geometrical center of mass M and m is equal to d , and $d \geq R$. Third test body is initially in the center of mass M , where also coordinate origin is placed. In co-rotating cartesian system (x, y) (cf. Fig. 1), equations of motion for third body, restricted to orbital plane, are:

$$\ddot{x} - 2\omega\dot{y} - kx + \frac{Gm(x-d)}{[(x-d)^2 + y^2]^{3/2}} + \frac{Gm}{d^2} = 0, \quad (1a)$$

$$\ddot{y} + 2\omega\dot{x} + ky + \frac{Gmy}{[(x-d)^2 + y^2]^{3/2}} = 0, \quad (1b)$$

where dot denotes time derivative, and, from Kepler law:

$$\omega^2 = \frac{G(m+M)}{d^3} \quad (2)$$

and:

$$k = \frac{4}{3}\pi G\rho - \omega^2. \quad (3)$$

System (1) is very similar to the classical planar restricted circular three body problem, see Capiski and Zgliczycki (2011). System (1), without terms *explicite* involving gravitational constant G , describe Foucault pendulum problem (Landau and Lifshitz 1969).

Conserved energy for system (1) is:

$$E = \frac{1}{2}\dot{x}^2 + \frac{1}{2}\dot{y}^2 + U(x, y), \quad (4a)$$

$$U = \frac{1}{2}k(x^2 + y^2) - \frac{Gm}{\sqrt{(x-d)^2 + y^2}} + \frac{Gm(x+d)}{d^2} \quad (4b)$$

Equations of motion (1) and energy (4b) with constant k are suitable for analysis of the small (linear) perturbations of the test body only. To explore non-linear effects, possible ejection of the test body from mass M in particular, we have to use model with non-constant density $\rho(r)$. This is done in Sect. 2.2.

Linearization of the equations (1) for small perturbations around point $x = 0, y = 0$ is done as follows. After substitution $x(t) = \epsilon\zeta(t), y(t) = \epsilon\xi(t)$ into (1), series expansion has been calculated with respect to ϵ , and higher-order terms dropped. Following linear system has been obtained:

$$\ddot{\zeta} - 2\omega\dot{\xi} + (k - 2q)\zeta = 0, \quad (5a)$$

$$\ddot{\xi} + 2\omega\dot{\zeta} + (k + q)\xi = 0, \quad (5b)$$

where:

$$q = \frac{Gm}{d^3}. \quad (6)$$

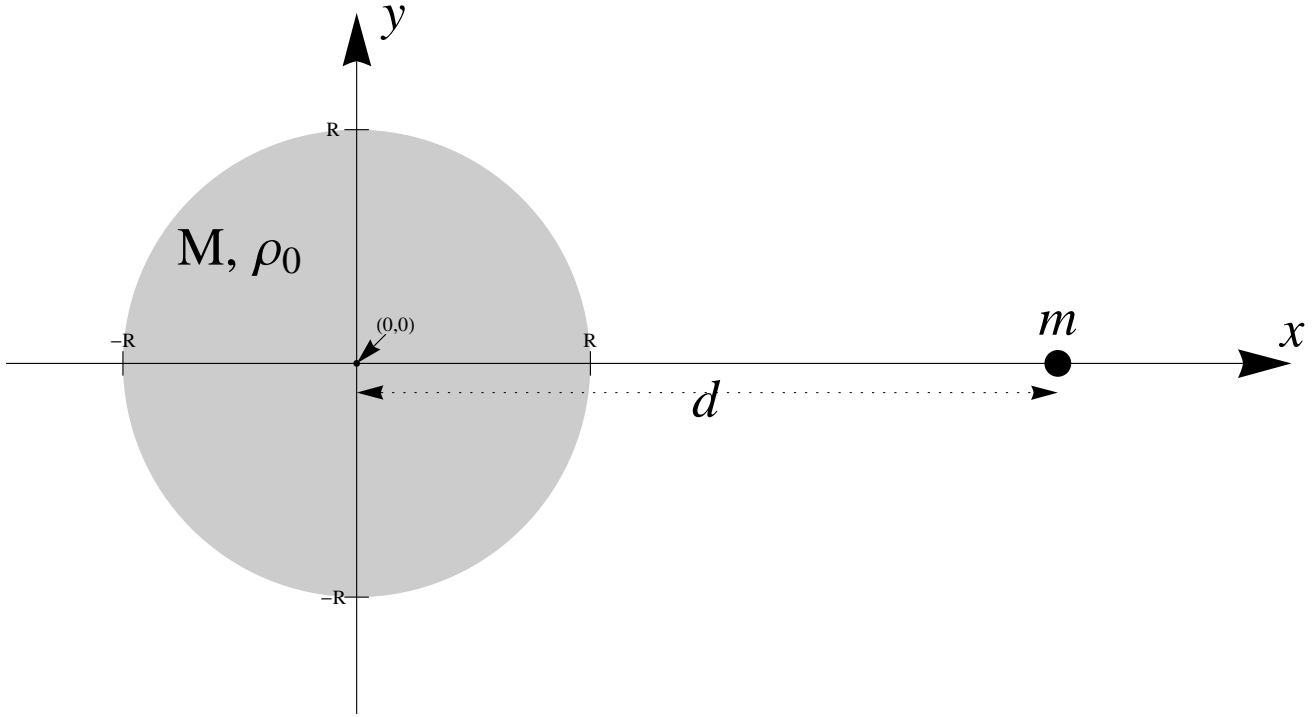


Figure 1. Co-rotating coordinate system used to derive (1).

Eigenvalues λ of the system (5) are solutions to the algebraic equation:

$$(\lambda^2 + k - 2q)(\lambda^2 + k + q) + 4\omega^2 = 0. \quad (7)$$

System is considered linearly unstable with respect to small perturbations if at least one solution of (7) has a positive real part:

$$Re(\lambda) > 0.$$

Resolving above conditions using quantifier elimination (Strzebonski 2000; Liska and Steinberg 1993) lead us to the instability criteria:

$$\frac{M}{d^3} < \frac{4}{3}\pi\rho < \frac{M+3m}{d^3}, \quad (8a)$$

$$\frac{4}{3}\pi\rho < \frac{1}{2} \frac{m}{d^3} \frac{M-m/8}{M+m}. \quad (8b)$$

Criteria (8) has been verified solving (1) numerically, and solving linearized system (5) analytically. Result (8a) can be obtained from analysis of the potential (4b) extremum at $x=0, y=0$ as well. Left-hand side of (8a), i.e., condition $M/d^3 < 4/3\pi\rho$, is trivial from astrophysical point of view, because the central density cannot be smaller than average density. In any realistic astronomical body, density decrease outwards: $\rho(r) \leq \rho(0)$. The same argument apply to (8b). Even in the most favorable situation $m=2M$, the central density should be less than half of the average density for mass m for this instability to occur¹.

If we assume, that density decreases outwards from the center,

we may simply write simplified form of (8), relevant to the astrophysical applications:

$$\frac{4}{3}\pi\rho < \frac{M+3m}{d^3}. \quad (9)$$

It is illustrative, to compare instability (9) with Roche limit (Chandrasekhar 1963; Gu et al. 2003). Let rewrite (9) as:

$$\frac{d}{R} < \left(1 + \frac{3m}{M}\right)^{1/3}. \quad (10)$$

Roche stability limit can be put in the form:

$$\frac{d}{R} > \kappa \left(\frac{m}{M}\right)^{1/3}, \quad (11)$$

where $\kappa = \sqrt[3]{3}$. Note, that for $m \gg M$ criteria (10) and (11) are asymptotically identical. Resonant instability (10) operates before Roche limit, leaving thin strip on $d/R - m/M$ plane, see Fig. 2. Depending on actual value of κ in (11), instability strip might widen if $\kappa < \sqrt[3]{3}$, or disappear completely for large m/M if $\kappa > \sqrt[3]{3}$. Only for $m/M < 1$ instability is always present before Roche limit. In other situations, mass M might be destroyed by tidal forces, before resonant instability takes its time. The latter require at least few orbital periods or more to be effective.

2.2 Numerical verification of the instability and the long-term behavior in non-linear regime

System (1) is a good tool to derive the instability criteria (8). For unstable cases point mass is likely to abandon central region. Whole density distribution $\rho(r)$, not just $\rho(0)$, becomes important. Location of "surface radius" defined as $\rho(R) = 0$ determine cases of "core ejection". Non-constant density cause harmonic oscillator

¹ However, artificial body with such properties could be created, and experiments performed in micro-gravity at orbital station.

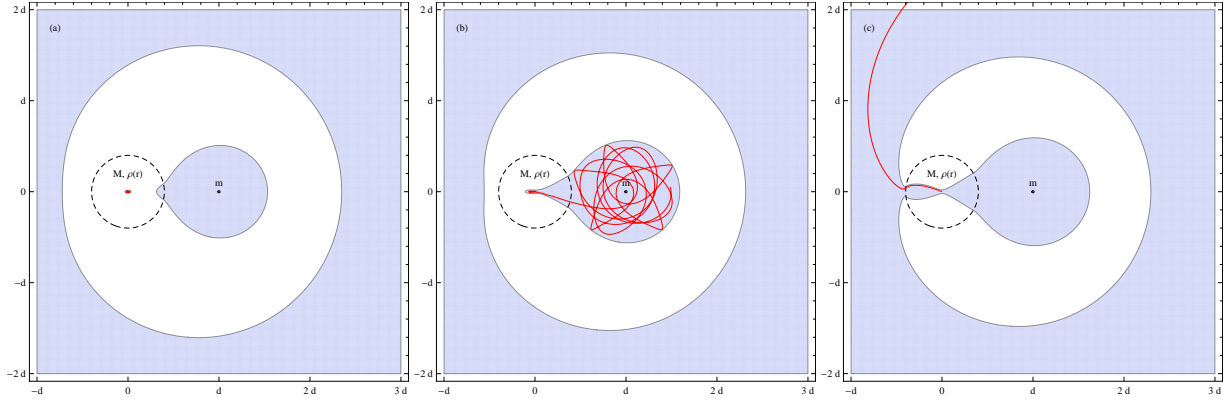


Figure 3. Three typical cases of the dynamics: stable (a), unstable chaotic (b), unstable with ejection (c). Gravitational potential of the uniform density ball (17) has been used to plot shaded region $U(x, y) < \delta E$ from (14).

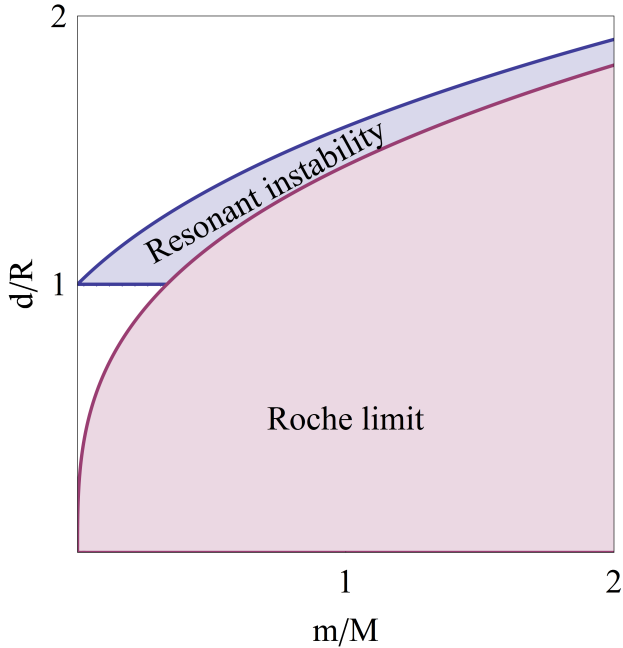


Figure 2. Sketch of the resonant instability region given by eq. (10), with Roche limit, eq. (11), superimposed on top. Blue strip marked "Resonant instability" shows parameter range, where phenomenon already operates, but mass M is still away from Roche boundary.

force change into more realistic, but also more complicated one. Introducing mass coordinate $m(r)$:

$$m(r) = 4\pi \int_0^r \rho(\zeta)\zeta^2 d\zeta$$

the system of equations of motion becomes similar to (1), but now $k = k(x, y)$:

$$k = \frac{Gm(r)}{r^3} - \omega^2, \quad r^2 = x^2 + y^2. \quad (12)$$

System (1) with non-constant $k(x, y)$ given by (12) is much more general, and cover astrophysically interesting cases with non-constant density.

Mass M is now equal to:

$$M \equiv m(R) = 4\pi \int_0^R \rho(\zeta)\zeta^2 d\zeta.$$

If we could allow mass m to orbit inside region where $\rho(r) > 0$, the inertial mass M_{inert} would become different than the gravitational mass M_{grav} . In such a situation, circular two-body problem has slightly different solution compared to classic one. Kepler frequency in particular is given by:

$$\omega^2 = G \frac{M_{grav} + m \frac{M_{grav}}{M_{inert}}}{d^3}. \quad (13)$$

I do not consider consequences of (13) further. I assume, that $R < d$, i.e., mass m orbits outside mass M .

For general $\rho(r)$ we still are able to derive conserved energy:

$$E = \frac{1}{2}\dot{x}^2 + \frac{1}{2}\dot{y}^2 + U(x, y) \quad (14a)$$

$$U = \phi(r) - \frac{1}{2}\omega^2 r^2 - \frac{Gm}{\sqrt{(x-d)^2 + y^2}} + \frac{Gm(x+d)}{d^2} \quad (14b)$$

where $r = \sqrt{x^2 + y^2}$ and:

$$\phi(r) = G \int_0^r \frac{m(\zeta)}{\zeta^2} d\zeta \quad (15)$$

is the gravitational potential of the star. For compatibility with (1) we choose $\phi(0) = 0$.

Simplest example, uniform density ball of radius R , leads to a piecewise-constant $\rho(r)$:

$$\rho(r) = \begin{cases} \rho_0 & \text{for } r < R \\ 0 & \text{for } r > R. \end{cases} \quad (16)$$

Gravitational potential for (16) calculated from (15) is:

$$\phi(r) = \begin{cases} \frac{2}{3}\pi G\rho_0 r^2 & \text{for } r < R \\ -\frac{GM}{r} + \frac{3}{2}\frac{GM}{R} & \text{for } r > R. \end{cases} \quad (17)$$

Before presentation of numerical calculations, it is desirable to understand possible trajectories qualitatively. Using energy considerations, we can find allowed regions on $x - y$ plane. Test body at rest in the central point $x = 0, y = 0$ has an energy of $E = 0$. Three typical cases are presented for uniform sphere of density ρ and radius R (dashed circle in Fig. 3). Energy had been perturbed with small positive value δE . Allowed Hill region:

$$U(x, y) < \delta E$$

has been shaded. In stable situation, see Fig. 3, panel (a), we have three disconnected regions: central area of mass M , neighborhood of mass m , and "outer space" extending to the infinity. Perturbed test body simply oscillates with frequency related to the central density, simultaneously rotating like Foucault pendulum. In the presence of the drag it will settle down at the geometrical center of mass M . When the density drops to a value below critical, given by eq. (9), central region of mass M and area surrounding mass m become connected, cf. Fig. 3, middle panel (b). Test body begin to oscillate with growing amplitude forced by gravitational pull of mass m . After some time, depending on amplitude of initial perturbation, test body is ejected from mass M and enter chaotic orbit around mass m , see Fig. 3, panel (b). It is still bounded with binary system. With density much smaller than critical, all three allowed regions become connected, and the test body will be ejected from the system, spiraling out into infinity (Fig. 3, panel c). Described behavior has been confirmed by the numerical solution of system (1) with non-constant k from eq. (12). Example trajectories for uniform density ball are shown in Fig. 3 using red curves.

Analyzed instability is not strictly resonant behavior with Kepler frequency (2), because instability criterion (8a) includes additional factor 3 before mass m . However, using language of resonances we can easily understand underlying physics (Mardling 2008b). Consider classical first-year student textbook example of uniform density ball with radius R and satellite in circular orbit just above surface ($d = R$). Well known result is that internal harmonic oscillator and orbital frequencies are identical. Therefore, test mass in the center is in resonance with small mass in orbit. However, astrophysical bodies are centrally condensed ($\rho_c > \bar{\rho}$) and binary companions are usually more distant ($d > R$), so this resonance disappear. But orbital frequency depends on both masses M and m . By adding mass to the system, in form of larger mass m , we can make these frequencies equal again. We have never assumed that mass M is dominant, so added mass m might be arbitrarily large.

Inevitable presence of dynamic drag inside gaseous objects (including GC, see Meylan and Heggie 1997) and other forms of friction forces acting on a test body inside mass M has surprisingly only a minor effect on resulting dynamics, at least in the framework of presented model. Drag suppress amplitude of oscillations and delay onset of the instability. However, in the resonant regime, point $x = 0, y = 0$ has a "top-hill" position in the potential landscape given by the equation (14b). In effect, the global dynamics remains the same. Numerical tests with simple drag of the form:

$$-\kappa(\rho)\dot{\mathbf{r}} \quad (18)$$

confirmed this, and revealed, that main effect is to delay onset of the instability until ejection from the system becomes possible, cf. Fig. 3, panel (c). Therefore, ejection is more likely outcome, while chaotic orbits (Fig. 3, panel (b)) might be rare. After test body leave mass M evolution is identical to the classical restricted planar circular three-body problem.

2.3 Three body instability

In this section I have removed assumptions of planar motion and negligible mass of the third body. Full system of nine equations describing motion of the three masses without additional simplifying assumptions can be transformed to the co-rotating system as well. Very lengthy calculations for full three body problem in three dimensions, show that criteria (8) nearly survive. Using quantifier

elimination for stability analysis of the linearized 18-order eigen-system we are able to show, that instability is present if:

$$\frac{M}{d^3} < \frac{4}{3}\pi\rho < \frac{M + 3m(1 + \mu/M)^{-1}}{d^3} \quad (19a)$$

$$\frac{4}{3}\pi\rho < \frac{1}{2}\frac{m}{d^3}\frac{M + \mu - m/8}{M + \mu + m}(1 + \mu/M)^{-1}. \quad (19b)$$

New factor in (19) is the mass of the third body equal to μ . For $\mu \rightarrow 0$, (19) reduces to (8).

Again, only (19a) is of astrophysical interest. Using orbital frequency:

$$\omega^2 = \frac{G(m + \mu + M)}{d^3}$$

and internal frequency:

$$\omega_c^2 = \frac{4}{3}\pi G \rho$$

we may write (19a) as:

$$\omega^2 + \frac{G(m + \mu)}{d^3} < \omega_c^2 < \omega^2 + \frac{G(m + \mu)}{d^3} + \frac{3Gm}{d^3}(1 + \mu/M)^{-1}.$$

Instability is a consequence of internal and orbital frequency overlap. Width of the resonance is proportional to „forcing” mass m , and reduced by factor dependent on mass ratio μ/M . The most important is magnitude of mass m , because it increase orbital frequency allowing for resonance. Simultaneously, it increase width of the instability window.

3 DISCUSSION OF POTENTIAL ASTROPHYSICAL SITES OF THE INSTABILITY

3.1 Massive binaries

Application of the results from Sect. 2.1 to a massive star is not straightforward, because „core” is not well-defined and separated from envelope. Red supergiants are indeed objects with nearly point-like core and extended low-density envelope. However, splitting radius is more or less arbitrary. It is also not clear what really will happen if instability becomes operational. Thorne-Zytkov objects are an exception, because central object is indeed well approximated by the point mass.

To overcome mentioned difficulties, I adopted the following procedure: star with total mass M_* and radius R_* is artificially divided into two parts: (i) central „core” region with $r < \xi$, and, (ii) outer envelope with $R_* > r > \xi$. Now, instability criteria (19) are functions of parameter ξ with:

$$\mu = \tilde{m}(\xi), \quad M = M_* - \tilde{m}(\xi), \quad \rho = \rho(\xi), \quad (20)$$

where $\tilde{m}(\xi)$ denotes mass enclosed by sphere with radius ξ . To further reduce complexity (dimensionality) of the analysis I assume that perturbing mass m is as close to star as possible, i.e., $d = R_*$. Stellar model s15 of Woosley et al. (2002) with mass $M_* = 12.8M_\odot$ and radius $R_* = 3.85AU$ at Si burning stage has been used as an example. The system is stable if:

$$\frac{4}{3}\pi\rho(\xi)R_*^3 > (M_* + 3m)\left(1 - \frac{\tilde{m}(\xi)}{M_*}\right). \quad (21)$$

In the above example „unstable core” has a minimal mass of $\simeq 4.3 M_\odot$. Noteworthy, edge of the He core is placed at $\simeq 4.2 M_\odot$. This result do not significantly vary within mass range $1 M_\odot < m < 100 M_\odot$. I conclude that splitting the red giant into helium

core and hydrogen envelope is the most appropriate. If we treat He core as a point mass, model presented in the article can be applied. It is likely, that during supernova event in close binary system, explosion engine will be displaced with respect to geometrical center of the hydrogen envelope. Recently discovered stripped helium core (low-mass white dwarf) in binary system (Maxted et al. 2011) might have been formed similar way.

3.2 Exoplanets and moons

Exoplanet formation and structure often consider compact core accreting mass in the form of extended low-density envelope (Laughlin et al. 2004). In this situation, dominant is the mass m , i.e., the central star, and instability occur if:

$$\frac{\rho}{1 \text{ g/cc}} \left(\frac{T}{1 \text{ day}} \right)^2 < 0.057 \frac{M_{env}}{M_{tot}}, \quad (22)$$

where: ρ is the density of the envelope, M_{env} is the mass of accreted envelope and M_{tot} is the total (core+envelope) mass of the protoplanet.

It is not surprising that all of the analyzed exoplanets are stable according to criterion (22). This is also true for so-called Ultra Short Period Planets (Sahu et al. 2006) with orbital period less than a day. However, stability margin is often small. We may speculate that some of the „puffy planets” (Hartman et al. 2011), i.e., very low density Jupiter-like objects close to the central star, were formed in process involving ejection of the dense planetary core due to instability presented in Sect. 2.3. Even if the instability do not lead to the core ejection due to, e.g., friction, dissipated energy might inflate the planet. This alone, however, does not explain lack of the rocky core.

3.3 Globular cluster

Galactic globular clusters are suspected to harbor intermediate-mass black hole in the center (Sun et al. 2013; Merritt 2013; den Brok et al. 2014). Therefore we can use above model to check if central position is stable with respect to perturbations caused by the Galaxy. Using database of Harris (1996, 2010 edition) and eq. (9) I have found that only few of GC are unstable, namely Lynga 7, FSR 1735, Terzan 4, 2MS-GC01, 2MS-GC02, BH 261, GLIMPSE02 and GLIMPSE01. In simulations of Lützendorf et al. (2013a) instability apparently has not appeared. It is not surprising due to resonant character of phenomena. It is unlikely to encounter such an instability for randomly chosen set of initial conditions. Very interesting is case of Terzan 3. It is stable if we put $m = 2 \times 10^{11} M_{\odot}$, i.e. mass of the Galaxy without dark matter (Sikora et al. 2012). However, if we include dark matter it becomes unstable. Therefore, the search for central black hole in Terzan 3 might provide falsification test for amount of the dark matter in the Galaxy. If the dark matter dominates mass of the Galaxy, IMBH in Terzan 3 must not exist. This requires further investigation, because orbits of GC are usually not circular, and Galaxy cannot be treated as a point mass. Another complication is caused by infinite radius of popular GC models, like Plummer sphere, see discussion related to (13). More detailed investigation of GC with IMBH and N-body validation of the model from Subsect. 2.3 is in progress.

3.4 LHC black hole

It has been speculated that LHC or other future high-energy experiment might produce artificial black hole, that do not explode

immediately *via* Hawking radiation (Casadio et al. 2010; Bleicher and Nicolini 2010; Gingrich 2010). Such a black hole would settle at central region of the Earth and slowly consume our home planet. I have applied instability criterion (9) to the Earth-Moon and Earth-Sun systems. Unfortunately, central position is stable by a wide margin in the sense of instability (8).

4 CONCLUSIONS AND DISCUSSION

Generalized three body model has been analyzed using analytical and numerical techniques. Instability of the point mass in the core-halo system was found. Analytical criteria (8) and (19) were derived using linearized system, and verified numerically.

Results were applied to astrophysical binaries, where one of the companions has a core-halo structure. Few possible sites for the instability were discussed: massive red supergiants in binary system (Subsect. 3.1), formation of the exoplanets (Subsect. 3.2) and globular clusters with intermediate black hole (Subsect. 3.3). Model can be applied to a more exotic situations, e.g., Thorne-Zytkov objects or central black holes of astrophysical and artificial origin as well.

Binary and multiple systems in astrophysics are rather a rule than exception, as well as core-halo structure of components, including dark matter halos and central black holes. Therefore, instability presented in the article might be of a very common occurrence in the nature, influencing formation and evolution of the astrophysical bodies and structures on various scales.

Derived results are very important. Simple analytical model provides input parameters for more advanced ones, numerical simulations in particular. Without such a guide, finding resonant behavior randomly sweeping parameter range is improbable. This is especially important for 3D simulations, which are limited by available computing power to just a few models (Handy et al. 2013).

In the real world, instability appears in situations, where perturbing mass m is either very close do mass M , or is much larger than mass M . If the former case it is likely, that mass m eventually enter into mass M , with dynamic drag causing inspiral, sweeping all orbital frequencies. Encountering instability conditions seems inevitable. However, reduced timescale available to system might prevent instability despite its exponential growth. If $m \gg M$ tidal effects are non-negligible, and instability asymptotically reduces to the Roche limit. Body with mass M might be destroyed by tidal forces, before resonant instability becomes operational. However, resonant instability appear before tidal disruption. Assumption of spherical symmetry and neglected rotation might lead to some additional effects, but usually spherical models are good enough to derive instability criteria.

Observational verification of the instability would be difficult in stars and planets, due to proximity of the Roche limit and complex hydrodynamics with similar timescales. For globular clusters, model looks essentially correct. Minor details like dynamic drag, non-circular orbits and finite size of the Galaxy are manageable, at least numerically. Unfortunately, existence of IMBH in the GC center is still under debate. Interesting option is an experimental verification of the instability at space station, using manufactured bodied in the form of, e.g., gas or liquid filled spheres or balloons.

Three body model needs to be validated. In particular, astrophysical bodies of interest are not rigid (typically gaseous, liquid or composed of particles), and might not react to a driving force as a whole. Ultimately, three dimensional hydrodynamic model with appropriate treatment of external gravity source, either analytical or

numerical, should be used to verify instability in binary stars. For globular clusters, N-body simulations provide a good framework to test model (work is in progress).

REFERENCES

- Arnett, W. D., Meakin, C., Jun. 2011. Toward Realistic Progenitors of Core-collapse Supernovae. *ApJ*733, 78–+.
- Bleicher, M., Nicolini, P., Jun. 2010. Large extra dimensions and small black holes at the LHC. *Journal of Physics Conference Series* 237 (1), 012008–+.
- Cannon, R. C., Aug. 1993. Massive Thorne-Zytkow Objects - Structure and Nucleosynthesis. *MNRAS*263, 817–+.
- Cannon, R. C., Eggleton, P. P., Zytow, A. N., Podsiadlowski, P., Feb. 1992. The structure and evolution of Thorne-Zytkow objects. *ApJ*386, 206–214.
- Capiski, M. J., Zgliczyski, P., 2011. Transition tori in the planar restricted elliptic three-body problem. *Nonlinearity* 24 (5), 1395. URL <http://stacks.iop.org/0951-7715/24/i=5/a=002>
- Casadio, R., Fabi, S., Harms, B., Micu, O., Feb. 2010. Theoretical survey of tidal-charged black holes at the LHC. *Journal of High Energy Physics* 2, 79–+.
- Chandrasekhar, S., Nov. 1963. The Equilibrium and the Stability of the Roche Ellipsoids. *ApJ*138, 1182.
- Clayton, D. D., Newman, M. J., Talbot, Jr., R. J., Oct. 1975. Solar models of low neutrino-counting rate - The central black hole. *ApJ*201, 489–493.
- den Brok, M., van de Ven, G., van den Bosch, R., Watkins, L., Feb. 2014. The central mass and mass-to-light profile of the Galactic globular cluster M15. *MNRAS*438, 487–493.
- Feldmeier, A., Lützgendorf, N., Neumayer, N., Kissler-Patig, M., Gebhardt, K., Baumgardt, H., Noyola, E., de Zeeuw, P. T., Jalali, B., Jun. 2013. Indication for an intermediate-mass black hole in the globular cluster NGC 5286 from kinematics. *A&A*554, A63.
- Gingrich, D. M., Mar. 2010. Production of tidal-charged black holes at the Large Hadron Collider. *Phys. Rev. D*81 (5), 057702–+.
- Gu, P.-G., Lin, D. N. C., Bodenheimer, P. H., May 2003. The Effect of Tidal Inflation Instability on the Mass and Dynamical Evolution of Extrasolar Planets with Ultrashort Periods. *ApJ*588, 509–534.
- Haghighipour, N., Sep. 2011. Super-Earths: a new class of planetary bodies. *Contemporary Physics* 52, 403–438.
- Handy, T., Plewa, T., Odrzywolek, A., Dec. 2013. Toward connecting core-collapse supernova theory with observations: I. Shock revival in a 15 Msun blue supergiant progenitor with SN 1987A energetics. *ArXiv e-prints*.
- Harris, W. E., Oct. 1996. A Catalog of Parameters for Globular Clusters in the Milky Way. *AJ*112, 1487.
- Hartman, J. D., Bakos, G. Á., Torres, G., Latham, D. W., Kovács, G., Béky, B., Quinn, S. N., Mazeh, T., Shporer, A., Marcy, G. W., Howard, A. W., Fischer, D. A., Johnson, J. A., Esquerdo, G. A., Noyes, R. W., Sasselov, D. D., Stefanik, R. P., Fernandez, J. M., Szklennár, T., Lázár, J., Papp, I., Sári, P., Nov. 2011. HAT-P-32b and HAT-P-33b: Two Highly Inflated Hot Jupiters Transiting High-jitter Stars. *ApJ*742, 59.
- Hawking, S., 1971. Gravitationally collapsed objects of very low mass. *MNRAS*152, 75–+.
- Hurđ, J.-M., Dieckmann, A., May 2012. A substitute for the singular Green kernel in the Newtonian potential of celestial bodies. *A&A*541, A130.
- Kuchner, M. J., Oct. 2003. Volatile-rich Earth-Mass Planets in the Habitable Zone. *ApJ*596, L105–L108.
- Landau, L. D., Lifshitz, E. M., 1969. *Mechanics*. Oxford: Pergamon Press, 1969, 2nd ed.
- Laughlin, G., Bodenheimer, P., Adams, F. C., 2004. The core accretion model predicts few jovian-mass planets orbiting red dwarfs. *The Astrophysical Journal Letters* 612 (1), L73. URL <http://stacks.iop.org/1538-4357/612/i=1/a=L73>
- Léger, A., Selsis, F., Sotin, C., Guillot, T., Despois, D., Mawet, D., Ollivier, M., Labèque, A., Valette, C., Brachet, F., Chazelas, B., Lammer, H., Jun. 2004. A new family of planets? “Ocean Planets”. *Icarus* 169, 499–504.
- Liska, R., Steinberg, S., 1993. Applying quantifier elimination to stability analysis of difference schemes. *The Computer Journal* 36 (5), 497–503. URL <http://comjnl.oxfordjournals.org/content/36/5/497.abstract>
- Lützgendorf, N., Baumgardt, H., Kruijssen, J. M. D., Oct. 2013a. N-body simulations of globular clusters in tidal fields: Effects of intermediate-mass black holes. *A&A*558, A117.
- Lützgendorf, N., Kissler-Patig, M., Gebhardt, K., Baumgardt, H., Noyola, E., de Zeeuw, P. T., Neumayer, N., Jalali, B., Feldmeier, A., 2013b. Intermediate-mass black holes in globular clusters. *Mem. Soc. Astron. Italiana*84, 129.
- Lützgendorf, N., Kissler-Patig, M., Gebhardt, K., Baumgardt, H., Noyola, E., de Zeeuw, P. T., Neumayer, N., Jalali, B., Feldmeier, A., Apr. 2013c. Limits on intermediate-mass black holes in six Galactic globular clusters with integral-field spectroscopy. *A&A*552, A49.
- Lützgendorf, N., Kissler-Patig, M., Neumayer, N., Baumgardt, H., Noyola, E., de Zeeuw, P. T., Gebhardt, K., Jalali, B., Feldmeier, A., Jul. 2013d. M - σ relation for intermediate-mass black holes in globular clusters. *A&A*555, A26.
- Mardling, R. A., 2008a. Resonance, Chaos and Stability: The Three-Body Problem in Astrophysics. In: S. J. Aarseth, C. A. Tout, & R. A. Mardling (Ed.), *The Cambridge N-Body Lectures*. Vol. 760 of *Lecture Notes in Physics*, Berlin Springer Verlag. pp. 59–96.
- Mardling, R. A., 2008b. Resonance, chaos and stability: The three-body problem in astrophysics. *Lecture Notes in Physics* 760, 59–96.
- Maxted, P. F. L., Anderson, D. R., Burleigh, M. R., Collier Cameron, A., Heber, U., Gänsicke, B. T., Geier, S., Kupfer, T., Marsh, T. R., Nelemans, G., O’Toole, S. J., Østensen, R. H., Smalley, B., West, R. G., Dec. 2011. Discovery of a stripped red giant core in a bright eclipsing binary system. *MNRAS*418, 1156–1164.
- Merritt, D., Jul. 2013. *Dynamics and Evolution of Galactic Nuclei*. Princeton University Press.
- Meylan, G., Heggie, D. C., 1997. Internal dynamics of globular clusters. *A&A Rev.*8, 1–143.
- Sahu, K. C., Casertano, S., Bond, H. E., Valenti, J., Ed Smith, T., Minniti, D., Zoccali, M., Livio, M., Panagia, N., Piskunov, N., Brown, T. M., Brown, T., Renzini, A., Rich, R. M., Clarkson, W., Lubow, S., Oct. 2006. Transiting extrasolar planetary candidates in the Galactic bulge. *Nature*443, 534–540.
- Sikora, S., Bratek, Ł., Jałocha, J., Kutschera, M., Oct. 2012. Gravitational microlensing as a test of a finite-width disk model of the Galaxy. *A&A*546, A126.

- Strzebonski, A., 2000. Solving algebraic inequalities. *Mathematica J.* 7, 525–541.
- Sun, M.-Y., Jin, Y.-L., Gu, W.-M., Liu, T., Lin, D.-B., Lu, J.-F., Oct. 2013. Do Intermediate-mass Black Holes Exist in Globular Clusters? *ApJ*776, 118.
- Thorne, K. S., Zytow, A. N., Mar. 1977. Stars with degenerate neutron cores. I - Structure of equilibrium models. *ApJ*212, 832–858.
- Umbreit, S., Rasio, F. A., May 2013. Constraining Intermediate-mass Black Holes in Globular Clusters. *ApJ*768, 26.
- Vanture, A. D., Zucker, D., Wallerstein, G., Apr. 1999. Is U Aquarii a Thorne-Zytow Object? *ApJ*514, 932–938.
- Wang, Y., Xu, S., 2013. Gravity gradient torque of spacecraft orbiting asteroids. *Aircraft Engineering and Aerospace Technology* 85 (1), 8–8.
- Woosley, S. E., Heger, A., Weaver, T. A., Nov. 2002. The evolution and explosion of massive stars. *Reviews of Modern Physics* 74, 1015–1071.